CRACK PROPAGATION IN FLEXURAL TESTING OF ADDITIVE MANUFACTURED ACRYLONITRILE BUTADIENE STYRENE

Y. Rosenthal[1], A. Stern[1], I. Treivish[2], D. Ashkenazi[3*]

[1]Afeka, Tel-Aviv Academic College of Engineering, Department of Mechanical Engineering, Tel Aviv 69107, Israel
[2]Nuclear Research Center - Negev, PO Box 9001, Beer Sheva 84190, Israel
[3]School of Mechanical Engineering, Tel Aviv University, Tel Aviv 6997801, Israel
*Corresponding author's e-mail address: dana@eng.tau.ac.il

ABSTRACT

Fused Deposition Modelling (FDM) is one of the most important Additive Manufacturing (AM) technologies. This is a technology suitable for various engineering applications and currently used with many types of thermoplastic materials including Acrylonitrile Butadiene Styrene (ABS). AM-FDM printed ABS possesses an inherent capacity for property modifications as a function of printing parameters. The main goal of the present ongoing research project is to estimate the strength of the AM-FDM printed ABS for varying printing process parameters. In the present study, the mechanical and structural characterizations of AM-FDM ABS were evaluated by light microscopy and mechanical testing. Three-point bend flexural test results revealed the mechanical properties as well as the fracture behaviour according to the dimensions and printing strategies of the build-on specimens. An innovative transmitted-light microscopy experimental method was developed and utilized to investigate the crack propagation behaviour under bending.

KEYWORDS: Additive manufacturing, FDM, ABS, Mechanical properties, Three-point bending flexural test, Crack propagation.

1. INTRODUCTION

One of the most important Additive Manufacturing (AM) technologies is the Fused Deposition Modelling (FDM), also known as fused filament fabrication (FFF), a technology suitable for various engineering applications, such as rapid prototyping, advanced composite parts and toys. FDM is currently used with many types of thermoplastic materials including Acrylonitrile Butadiene Styrene (ABS) [1]-[4]. AM-FDM printed ABS possesses an inherent capacity for property modifications as a function of building parameters. The ABS parts, produced by AM, display good chemical resistance, stable product dimensions, and good impact resistance. However, the same parts often have dissimilar mechanical behaviour when 3D printed in different orientations [5]-[7]. While FDM is one of the most commonly used AM technologies for modelling, prototyping, and selected structural applications, the major research inquiries have revolved around balancing the ability to produce aesthetically appealing looking products without compromising functionality. When it comes to components' functionality, structural integrity (preventing fracture) is of the highest importance.

The relationship between mechanical properties and fracture morphology of ABS material and FDM process parameters has been studied in the last years by several research groups [8]-[19]. Printed ABS standard tensile specimens (ASTM D638, Type V) demonstrate a "ductile" fracture morphology [17], [20]-[23]. The tensile strength, compressive strength, and flexural bending strength, together with the fracture appearance of ABS specimens, were investigated as a function of process parameters such as specimen temperature, specimen orientation, the quality of polymer filament, layer thickness, air gap, raster orientation, and raster width [17], [20]-[23].

The present study evaluates the relationship between the mechanical properties in bending and the structural characteristics of FDM ABS material, using different building strategies. The mechanical properties of FDM parts are not solely controlled by the material of the original filament but are also significantly influenced by a directionally dependent production process that fabricates components with anisotropic characteristics associated with the inherent layering, and finally by the loading conditions in service. The crack propagation behaviour in ABS under three-point bending loads was characterized as

Date of submission/acceptance: 24.12.2018/15.12.2019 https://doi.org/10.35219/awet.2019.03

part of an ongoing research project on AM-FDM printed ABS for various modelling purposes. In this experimental study, the mechanical and structural features in various building orientations were obtained through flexural testing (ASTM D790). Transmitted light microscopy was used to reveal stressed and deformed layers governing the crack propagation. The results can contribute to better and faster analysis capability of the output data for modelling purposes and understanding the fracture modes of ABS in flexural tests.

2. EXPERIMENTAL PART

2.1. Material and FDM Process

All ABS specimens were designed with computed aided design (CAD), using SolidWorks 2017 program, and were built with a STRATASYS© Dimension Elite FDM™ machine (Fig. 1) system [10], [20], [23]. The maximum extrusion temperature was ~ 285 ºC, the building chamber temperature was ~ 70 ºC, and the nozzle speed during extrusion was up to 12.7 mm/sec [20]. There are three available material filling options for this system (low density, high density and solid). The specimens of the present research were printed in low density (50% of the volume) and solid (100% of the volume) filling modes. The molten ABS layers built across the tray were directed in ±45º in relation to the X-axis.

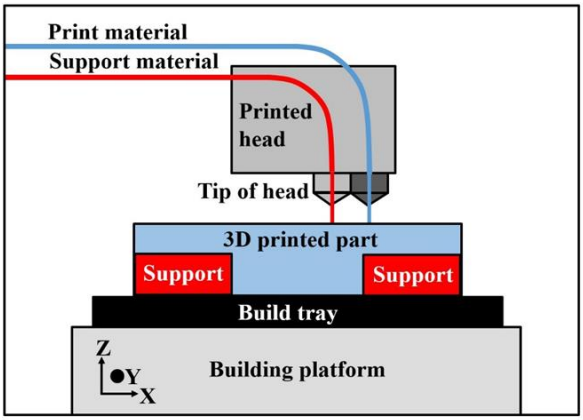

Fig. 1. Schematic illustration [4], [10] of the AM-FDM technology. The main parts of the 3D printing machine are shown as well as the direction of the printed molten ABS filament's configuration

2.2. Specimens

Standard three-point bending specimens in accordance with the ASTM D790 standards were additively manufactured (3 trays) with different printing parameters and various orientation groups (Fig. 2). Bending specimens with their length printed in the Y-Axis and width parallel to the X-axis were used for the crack propagation research.

2.3. Three-Point Bending Test System Setup

The bending tests were conducted using an MTS© Model E43-504 universal testing machine equipped with a three-point bending fixture (Fig. 3). A Crosshead velocity of 0.5 mm min^{-1} was used for all tests. Based on the theory of force and internal moment generated on a loaded beam, the flexural strength σ_b was calculated from Eq. (1):

$$\sigma = \frac{3f \cdot L}{2b \cdot h^2} \quad (1)$$

where f is the applied force, L is the span between the two anvils, and b and h are the measured dimensions of the specimen's cross-section.

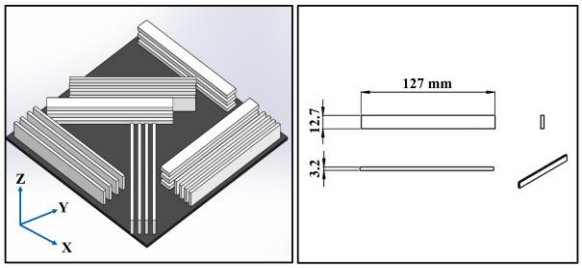

(a) (b)

Fig. 2. The printed ABS specimens and building orientations: (a) an illustration of a typical printing tray design showing the main axes; (b) a drawing of the tested three-point bending test specimen

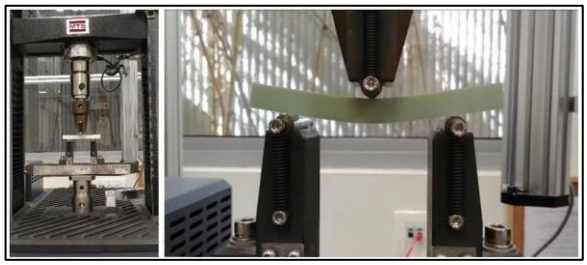

(a) (b)

Fig. 3. The experimental setup; (a) a general view of the three-point bending fixture attached to the testing machine; (b) close-up of the three-point bending bridge; the span L is 80 mm

As mentioned above, bending specimens with their length printed in the Y-Axis direction and their width parallel to the X-axis direction were used for the crack propagation research. These specimens were loaded in the X-axis direction to evaluate the interaction of the propagating crack with printed ABS layers printed at an angle of 45º to the loading line.

2.4. Fractography

Nikon© SMZ800 Zoom Stereomicroscope was used (a) for surface observation; (b) to perform

fractographic examinations of fracture face morphology ("ductile", "brittle" or "mixed mode") following the mechanical tests and; (c) to find any possible defects that might affect the quality of the printed specimens' properties.

2.5. Transmitted-Light Fractography

A new experimental method was developed to examine and visualize the specimens' surface and the in-depth phenomenon in the surroundings of the propagated crack. The observation system consists of an Olympus© BX43 biological computerized microscope equipped with an Olympus© DP73 camera, controlled using cellSense Entry 1.9 program (Copyright ©2009-2013 Olympus Corporation). Transmitted light (sometimes called transillumination) shines light from a transmitted-light illuminator and through the specimen to the viewing lens. It is used for transparent or translucent objects, commonly found in prepared biological specimens (e.g., slides), or with thin sections of otherwise opaque materials such as mineral specimens.

3. RESULTS AND DISCUSSION

3.1. Three-Point Bending Mechanical Properties

The mechanical properties obtained from the three-point bending experimental tests, compiled from three building trays, are shown in Fig. 4. (a) Flexural stress is commonly used, instead of load values, as per ASTM D790 that provides the way to report the three-point bending test results (see also eq. 1 in the paper); (b) bending was conducted at a constant crosshead velocity – 0.5 mm min^{-1}, that can be used, along with axial deflection data to obtain the test time; and (c) the deflection values presented in Fig. 4b correspond to the initiation of crack propagation. The mechanical testing results of specimens from the first tray show significant differences between the X-axis and Z-axis specimens. The flexural strength of the X-axis specimens shows about ~ 2.2 times greater values than the flexural strength of the Z-axis specimens. Fig. 4 presents the flexural strength and deflection data for all three batches of specimens manufactured in X and Z directions and tested in bending. The difference between flexural strength values in the X-axis vs Z axis was highlighted as the most observed phenomenon. The axial displacement (deflection) values of the X-axis specimens are also greater than the deflection of the Z-axis specimens. Specimens built in the X direction, 45° orientation, have slightly higher flexural strength and deflection values than the specimens built in the X-axis orientation.

The flexural strength of the X-axis specimens from the second tray shows about ~ 2.8 times greater value than the flexural strength of the Z-axis specimens. The deflection in the X-axis specimens is also greater than that of the Z-axis specimens. Specimens built in the X-axis, 45° orientation, have slightly higher flexural strength and deflection values than those obtained from the specimens built in the X-axis orientation. There is no significant difference in the flexural strength of these specimens, in comparison to the specimens in the first tray.

For specimens from the third tray, the flexural strength of the X-axis specimens shows about ~ 2 times greater value than the strength of the Z-axis specimens. The deflection in the X-axis specimens is also greater than that of the Z-axis specimens. Specimens built in the X-axis orientation have slightly higher strength values than those built in the X-axis, 45° orientation, as opposed to the first and second trays. Additionally, a comparison of the third tray with the first and second trays, indicates a decrease in the flexural strength of the specimens from the third tray.

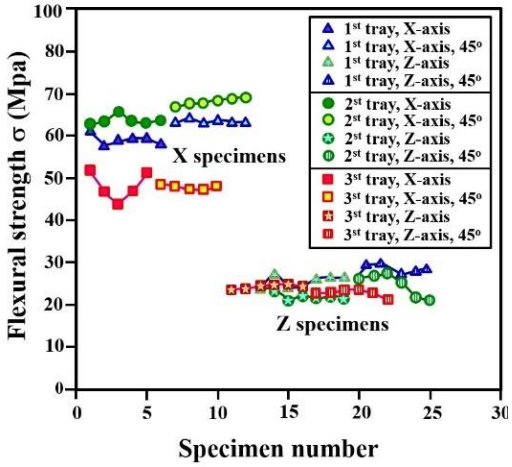

(a)

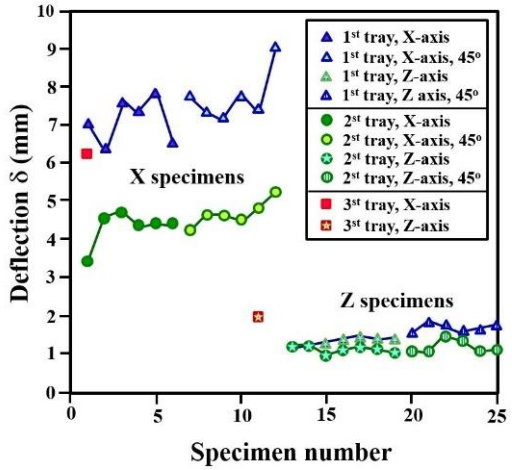

(b)

Fig. 4. Experimental results for three batches (a batch consists of the specimens printed on one tray), showing (a) the values of the flexural strength, and, (b) the values of the axial deflection (printing density and layer thickness were changed in tray 3 and the results are given for comparison purposes)

3.2. Fractography

3.2.1. Deformation Bands near the Crack Path

During the bending tests we closely watched the specimens for any irregularities or any unusual phenomena. The bending tests were stopped just before the final failure to allow for clear and complete examination of the specimens' surfaces as well as the crack and its surroundings. It was observed, for all specimens printed in the X-axis orientation, that when the bending test reaches a point involving large axial displacement (large deflection), the outer layers fail, and a crack starts to propagate from the lower side (where tensile stresses are dominant) upwards. Following the crack propagation, a symmetric pattern of straight lines, having different lengths, is formed and appears on both sides of the crack, about 10 mm on each side (Fig. 5). The lines are spaced equally around the crack path. The distance between the lines is about 0.1 mm, and their length changes linearly, forming a triangular pattern on both sides of the crack path.

These lines are assumed to be deformation bands where their length can be related to the stress field magnitudes formed around the crack.

If the assumption is that triangular patterns represent the stress fields around the crack, then their length and location are governed by the tensile and shear stress distribution within the specimen. The bright area observed at the upper point of the triangular pattern can be assumed to be the stress field ahead of the crack tip. This controls the crack propagation behaviour. Similar patterns, in crack mouth opening displacement specimens, were reported by N. Patel and B. Patel [24] in their analysis of FDM manufactured ABS using FEM.

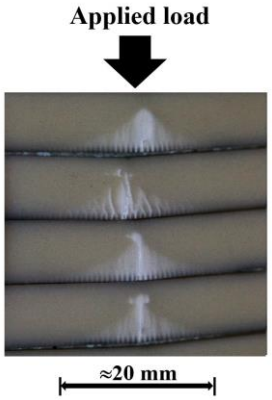

Fig. 5. The typical symmetric pattern of straight lines, having different lengths, on both sides of the propagated crack is shown here (the bending test was stopped just before the final failure to allow for complete view of the line patterns; the straight lines are assumed to be deformation bands; stress fields are visible ahead of the crack tip)

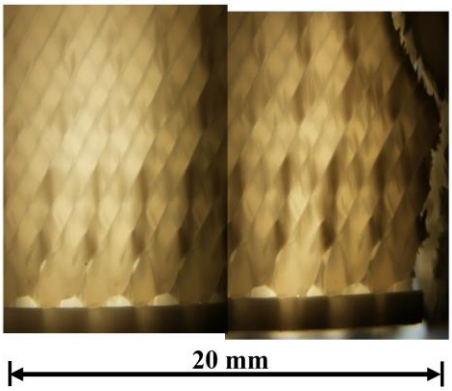

Fig. 6. Transmitted light microcopy enabled the visual observation of the symmetrically deformed structure, near the crack initiation (the crack initiation and propagation affect only the areas located 10 mm from both sides of its path; the length of the deformed stripes - can be a measure for the magnitude of the local stress fields - changes linearly throughout this distance)

3.2.2. Interactions of the Crack and the X-axis ABS Structure

As previously described, the formation of a triangular pattern consisting of different-length stripes was visually observed by the naked eye and with a stereoscope (Fig. 5). These patterns appeared on both sides of the crack, propagating from the lower part of the specimen upwards. Due to the triangular pattern along with its incident crack path's resemblance to the stress field applied by a crack during its propagation, we have intuitively nicknamed these stripes "deformation bands".

Following this, the specimens were observed utilizing a biological microscope system, equipped with an illuminator and a light beam that is transmitted through the half-translucent specimens. It was immediately noticeable (Fig. 6) that the straight stripes that were previously observed account for the built layers stemming from the building strategy of the ABS material and FDM process (X-built specimens). These layers underwent deformation proportional to their distance from the crack propagating through the built layers and the stress fields that are formed (Fig. 7). The height of the deformed layers in relation to the distance from both sides of the crack, decreasing symmetrically in nature, provides a visual concept for the stress distribution. Only through the adaptation of proper technology and equipment typically used in the Biological field were we able to interpret the visual meaning of the above-mentioned stripes. The transmitted light scatters and is reflected in different directions while incidence with the deformed layers leads to their highlighting, thus providing the interpretation explained in this work. Further work will emphasize the quantitative correlation between the size and location of the stripes with the stress fields and deformations of the flexural

tests. ABS is usually used in making smaller models for structures, and this work can be used to understand the basic elements of material-crack interactions/propagations due to external loads.

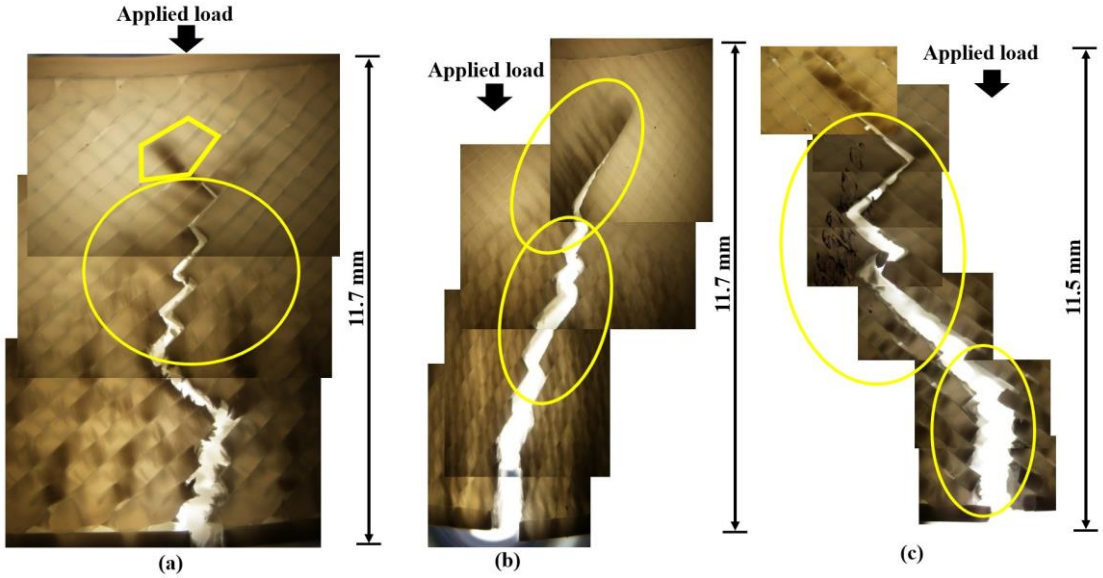

Fig. 7. Photographic sequences, utilizing the transmitted - light microscopy system showing the crack propagation behaviour and its interaction throughout the width of the printed ABS bending specimen, stopped just prior to complete failure: a) following initiation at a point of maximum tensile stress, the crack cuts through the first 3-4 printed layers and then, because of the stress level and deformed layer, jumps through 5 layers; just prior to complete failure the crack narrows and propagates through the layer borders being the weakest link; stress fields are observed ahead of the crack tip; b) highlight of a massive stress field on one side of the narrow crack, 3 layers before failure; c) different specimens showing combinations of the phenomenon observed in a) and b)

4. CONCLUSIONS

The mechanical and structural characterization of AM-FDM printed ABS material was performed using three-point bending specimens built in different building orientations and printing parameters. The mechanical testing results provided quantitative estimates for the flexural strength and fracture morphology as a function of the applied AM-FDM process parameters. The flexural strength values of the X-axis specimens are about ~ 2.2 times greater than the flexural strength values of the Z-axis specimens.

A new experimental method was developed to examine and visualize the specimens' surface and the in-depth phenomena in the vicinity of the propagated crack. The crack propagation behaviour in ABS under bending loads was characterized. We examined the results of interaction of the propagated crack with the ABS layered structure and sub-structure. Deformed and stressed layers and stress fields were observed and located with respect to the crack path during the test.

Further work will emphasize the quantitative correlation between the size and location of the observed stripe patterns with the stress fields and deformations of the flexural tests. This work can be used to understand the basic elements of material-crack interactions/propagations due to external loads.

NOMENCLATURE

F	-	applied bending load
L	-	span of the bending bridge
b	-	width of the bending specimen
h	-	height of the bending specimen
σ	-	flexural strength
δ	-	axial deflection

ACKNOWLEDGEMENTS

The authors would like to acknowledge the work of Avital Solomon, Naveh Dresler, Dor Shabat, Erez Shprontz, and Sagi Sigler from the Afeka college of Engineering. The assistance of Asher Tourgeman from the NRCN is highly appreciated. Many thanks to Ronit Ben-Romano and Drora Chayun from the Medical Faculty Labs., Soroka Hospital/Ben Gurion Univ., Beer Sheva. We deeply appreciate Idan Rosenthal, from the Ben-Gurion University, for fruitful discussions and assistance.

REFERENCES

[1] **Ngo T. D., Kashani A., Imbalzano G., Nguyen K. T., Hui D.**, *Additive manufacturing (3D printing): A review of materials, methods, applications and challenges*, Composites Part B: Engineering 143, 2018, pp. 172–196.

[2] **Rios O., Carter W., Post B., Lloyd P., Fenn D., Kutchko C., Rock R., Olson K., Compton B.**, *3D printing via ambient*

reactive extrusion, Materials Today Communications, 15, 2018, pp. 333–336.
[3] **Singh S., Ramakrishna S., Singh R.**, *Material issues in additive manufacturing: A review*, Journal of Manufacturing Processes 25, 2017, pp. 185–200.
[4] **Wong K. V., Hernandez A.**, *A review of additive manufacturing*, ISRN Mechanical Engineering, 2012, pp. 1–11.
[5] **Balderrama-Armendariz C. O., MacDonald E., Esplin D., Cortes-Saenz D., Wicker R., Maldonado-Macias A.**, *Torsion analysis of the anisotropic behavior of FDM technology*, The International Journal of Advanced Manufacturing Technology 96, 2018, pp. 307–317.
[6] **Costabile G., Fera M., Fruggiero F., Lambiase A., Pham, D.**, *Cost models of additive manufacturing: A literature review*, International Journal of Industrial Engineering Computations 8.2, 2017, pp. 263–283.
[7] **Li G., Zhao J., Wu W., Jiang J., Wang B., Jiang H., Fuh J. Y. H.**, *Effect of ultrasonic vibration on mechanical properties of 3D printing non-crystalline and semi-crystalline polymers*, Materials 11.5, 2018, pp. 826–839.
[8] **Jin Y. A., He Y., Fu J. Z., Gan W. F. Lin, Z. W.,** *Optimization of tool-path generation for material extrusion-based additive manufacturing technology*, Additive Manufacturing 1, 2014, pp. 32–47.
[9] **Wu W., Geng P., Li G., Zhao D., Zhang H., Zhao J.**, *Influence of layer thickness and raster angle on the mechanical properties of 3D-printed PEEK and a comparative mechanical study between PEEK and ABS*, Materials 8.9, 2015, pp. 5834–5846.
[10] **Magalhães L. C., Volpato N., Luersen M.**, *Build parameters influence on FDM parts mechanical behavior*, 21st Brazilian Congress of Mechanical Engineering, October 2011, Natal, RN, Brazil, pp. 24–28.
[11] **Tymrak B. M., Kreiger M., Pearce J. M.**, *Mechanical properties of components fabricated with open-source 3-D printers under realistic environmental conditions*, Materials & Design 58, 2014, pp. 242–246.
[12] **Durgun I., Ertan R.**, *Experimental investigation of FDM process for improvement of mechanical properties and production cost*, Rapid Prototyping Journal 20.3, 2014, pp. 228–235.
[13] **Hossain M. S., Ramos J., Espalin D., Perez M., Wicker R.**, *Improving tensile mechanical properties of FDM-manufactured specimens via modifying build parameters*, In International Solid Freeform Fabrication Symposium: An Additive Manufacturing Conference, 2013, Austin, TX, pp. 380–392.
[14] **Qureshi A. J., Mahmood S., Wong W. L. E., Talamona D.**, *Design for Scalability and Strength Optimisation for components created through FDM process*, Proceedings of the 20th International Conference on Engineering Design 6, 2015, pp. 255–266.
[15] **Górski F., Wichniarek R., Kuczko W., Zawadzki P., Buń P.**, *Strength of ABS parts produced by Fused Deposition Modelling technology–a critical orientation problem*, Advances in Science and Technology Research Journal 9.26, 2015, pp. 12–19.
[16] **Vairis A., Petousis M., Vidakis N., Savvakis K.**, *On the Strain Rate Sensitivity of ABS and ABS Plus Fused Deposition Modeling Parts*, Journal of Materials Engineering and Performance *25*.9, 2016, pp. 3558–3565.
[17] **Torrado A. R., Shemelya C. M., English J. D., Lin Y., Wicker R. B., Roberson D. A.**, *Characterizing the effect of additives to ABS on the mechanical property anisotropy of specimens fabricated by material extrusion 3D printing*, Additive Manufacturing 6, 2015, pp. 16–29.
[18] **Torrado A. R., Roberson D. A.**, *Failure analysis and anisotropy evaluation of 3D-printed tensile test specimens of different geometries and print raster patterns*, Journal of Failure Analysis and Prevention 16.1, 2016, pp. 154–164.
[19] **Zhang Y., Chou K.**, *A parametric study of part distortions in fused deposition modelling using three-dimensional finite element analysis*, Proceedings of the Institution of Mechanical Engineers, Part B: Journal of Engineering Manufacture 222(8), 2008, pp. 959–968.
[20] **Shabat D., Rosenthal Y., Ashkenazi D., Stern A.**, *Mechanical and structural characteristics of fused deposition modeling ABS material*, The Annals of "Dunarea De Jos" University of Galati. Fascicle XII: Welding Equipment and Technology 28, 2017, pp.16–24.
[21] **Siqueiros J. G., Schnittker K., Roberson D. A.,** *ABS-malleated SEBS blend as a 3D printable material*, Virtual and Physical Prototyping 11.2, 2016, pp. 123–131.
[22] **Perez A. R. T., Roberson D. A., Wicker R. B.**, *Fracture surface analysis of 3D-printed tensile specimens of novel ABS-based materials*, Journal of Failure Analysis and Prevention 14.3, 2014, pp. 343–353.
[23] **Berger A., Sharon Y., Ashkenazi D., Stern A.,** *Test artifact for additive manufacturing technology: FDM and SLM preliminary results*, The Annals of "Dunarea De Jos" University of Galati Fascicle XII, Welding Equipment and Technology 27, 2016, pp. 29–37.
[24] **Patel N., Patel B.**, *Fracture analysis of FDM manufactured ABS using FEM*, IJRRCME, Vol.2, Issue 1, pp. 84–90, April-Sept. 2015.